Parkinson CL (1997) *Earth from Above: Using Color-Coded Satellite Images to Examine the Global Environment*. Sausalito, CA: University Science Books.

Parkinson CL (2000) Variability of Arctic sea ice: the view from space, an 18-year record. *Arctic* 53(4): 341–358.

Smith WO Jr and Grebmeier JM (eds) (1995) *Arctic Oceanography: Marginal Ice Zones and Continental Shelves*. Washington, DC: American Geophysical Union.

Ulaby FT, Moore RK and Fung AK (1986) Monitoring sea ice. In: *Microwave Remote Sensing: Active and Passive, Vol. III: From Theory to Applications*, pp. 1478–1521. Dedham, MA: Artech House.

SATELLITE REMOTE SENSING MICROWAVE SCATTEROMETERS

W. J. Plant, Applied Physics Laboratory, University of Washington, Seattle, WA, USA

doi:10.1006/rwos.2001.0337

Introduction

Microwave scatterometers are instruments that transmit low-power pulses of radiation toward the Earth's surface at intermediate incidence angles and measure the intensity of the signals scattered back at the same angles from surface areas a few kilometers on a side. Satellite scatterometers operate continuously and therefore scatter from land and ice as well as the ocean. Useful information is available in the signals from land and ice, but will not be discussed here. This article will concentrate on the primary goal of satellite scatterometers: the measurement of near-surface wind speed and direction over the ocean.

Scatterometers achieve this goal by measuring the intensity, or cross-section, of microwave signals backscattered from the ocean surface. Common frequencies of the transmitted signals for satellite scatterometers are near 5.3 GHz (C-band) on European instruments and 14 GHz (Ku-band) on US ones. At these frequencies, microwaves penetrate only a few millimeters into sea water, so all backscatter originates at the surface and is caused by the roughness of the surface; a perfectly calm sea surface produces no detectable scattering in the direction of the incident radiation. Changes in the average roughness of the ocean surface over scales of several kilometers are caused primarily, but not exclusively, by changes in the wind speed or direction at the ocean surface. Standard assumptions of scatterometry are that the backscatter cross-section, usually called σ_o, over such scales depends only on parameters of the scatterometer and on the mean wind, increases with wind speed, is a maximum when the antenna looks upwind, and is a minimum when the antenna looks nearly perpendicular to the wind, or crosswind. These assumptions allow the wind speed and direction to be determined from cross-sections measured for the same patch of the ocean, but with the antenna directed at several different azimuth angles. For satellite scatterometry a given patch of ocean can be viewed from several different directions only by allowing the scatterometer to sweep its antenna beams across the patch, a process that requires as much as 4 min. Thus an additional assumption of scatterometry is that average winds over kilometer-scale patches of ocean surface are stationary for several minutes.

With these assumptions and an adequate definition of the wind being measured (discussed below), satellite scatterometers have proven to be able to measure winds over the ocean with accuracies as good as or better than *in situ* measurement techniques. Because oceans cover most of the Earth, this means that microwave scatterometers carried on satellites can monitor the wind field over most of the globe every few days. **Table 1** gives typical specifications that a satellite scatterometer can be expected to meet.

The spatial coverage offered by satellite scatterometry is far better than can be achieved by *in situ* measurements. It allows scatterometers to provide data to study global weather patterns,

Table 1 Expected specifications of the NSCAT satellite scatterometer

Parameter	*Value*	*Accuracy/comment*
Wind speed	3–30 m s^{-1}	2 m s^{-1} or 10%
Wind direction	3–30 m s^{-1}	20°
Spatial resolution	50 km	Wind cells
Location accuracy	25/10 km	Absolute/relative
Coverage	90% of ice-free ocean	Every 2 d
Mission duration	3 y	Includes check out

(Data from Naderi *et al.* 1991.)

Table 2 Scatterometers in space to date and planned for the future

Satellite	*Country/agency*	*Scatterometer*	*Launch date*	*Status*
Seasat	USA/NASA	SASS	June 1978	Failed, October 1978
ERS-1	Europe/ESA	CSCAT(AMI)	July 1991	Standby, June 1996
ERS-2	Europe/ESA	CSCAT(AMI)	April 1995	Operational
ADEOS-I	USA/NASA Japan/NASDA	NSCAT	August 1996	ADEOS failed June 1997
QuikSCAT	USA/NASA	SeaWinds-1	June 1999	Operational
ADEOS-II	USA/NASA Japan/NASDA	SeaWinds-2	November 2001	Approved
ASCAT	Europe/ESA	Adv.CSCAT	2003	Proposed

(Adapted from Patzert and Van Woert, private communication.)

monitor storm intensities, improve meteorological forecasts, impact global ocean circulation models, facilitate climate prediction, and much more. In addition to introducing the basics of scatterometry, this article will provide examples of these benefits of satellite scatterometry and indicate how continued improvements in the technique may be expected to provide even better results in the future.

Satellite Scatterometers

Other instruments such as radar altimeters that look straight down and real and synthetic aperture radars (RARs and SARs) that image surface scenes at resolutions of meters to kilometers have been operated in space and are capable of measuring wind speed or direction, but not both simultaneously and routinely. Microwave radiometers, passive instruments that measure the naturally occurring radiation from the ocean surface, are presently being developed as spaceborne anemometers capable of measuring wind speed and direction simultaneously. However, only microwave scatterometers, active instruments that both transmit and receive radiation, have a history of wind vector measurement from space. Because they are microwave, scatterometers can make their measurements both day and night and in most kinds of weather. Only very heavy rainfall, as discussed below, can hinder a scatterometer's view of the surface.

For these reasons, microwave scatterometers have been the instruments of choice for measuring near-surface winds from space. **Table 2** lists the scatterometers that have been in space to date and those that are planned for the future. As the table shows, the first scatterometer in space specifically designed to measure winds was the one on Seasat in 1978. An earlier microwave radar on Skylab viewed the ocean surface at intermediate incidence angles from space in 1973, but did not produce multiple looks at a single ocean patch from which wind vector information could be obtained. With the launch of the C-band scatterometer on the first European Remote Sensing Satellite (ERS-1) in 1991, a continuous series of global wind vector measurements was begun. As **Table 2** shows, this series has continued to the present through the launch of ERS-2 and the subsequent decommissioning of ERS-1. If present plans are carried out, at least two microwave scatterometers (and one or more microwave radiometers) will continue to produce global wind vector information into the foreseeable future.

While most scatterometers in space have consisted of multiple, fixed waveguide (stick) antennas, more recent US scatterometers have used rotating parabolic antennas. All satellite scatterometers to date have been in orbits with inclinations near 98.5°, except for Seasat which was 108°. Spatial resolutions have usually been 50×50 km, although 25×25 km is becoming more common. **Table 3**

Table 3 Principal characteristics of satellite scatterometers

Satellite	*Type*	*Frequency (GHz)*	*Polarization*	*Incidence angle (°)*	*Swath (km)*	*Altitude (km)*
Seasat	4 stick	14.6	4 VV, 4 HH	25–55 0–4	475, 475 140	800
ERS-1	3 stick	5.3	3 VV	18–57	500	785
ERS-2	3 stick	5.3	3 VV	18–57	500	785
ADEOS-I	6 stick	14.0	6 VV, 2 HH	15–63	600, 600	797
QuikSCAT	1 rotating	13.4	1 VV, 1 HH	46(H), 54(V)	1800	803
ADEOS-II	1 rotating	13.4	1 VV, 1 HH	46(H), 54(V)	1800	803
METOP	3 stick	–	–	–	–	835

addresses the primary characteristics of the scatterometers listed in **Table 2**. As **Table 3** shows, ERS scatterometers have had about half the spatial coverage of their NASA counterparts because their antennas view only one side of the subsatellite path. As discussed below, however, uniformly reliable wind vectors are not obtained over the whole swath of the SeaWinds instruments. Also a gap is present between the two swaths on either side of the subsatellite path of the NASA stick-type scatterometers because the response of the cross-section to the wind vector is weak at low incidence angles. The Seasat scatterometer did have a mode that observed the surface at very low incidence angles, but could not get wind direction in this swath without extrapolation from the wider swaths. **Figure 1** shows the fixed-stick ERS-1 scatterometer (**Figure 1A**) and the rotating-antenna QuickSCAT scatterometer (**Figure 1B**).

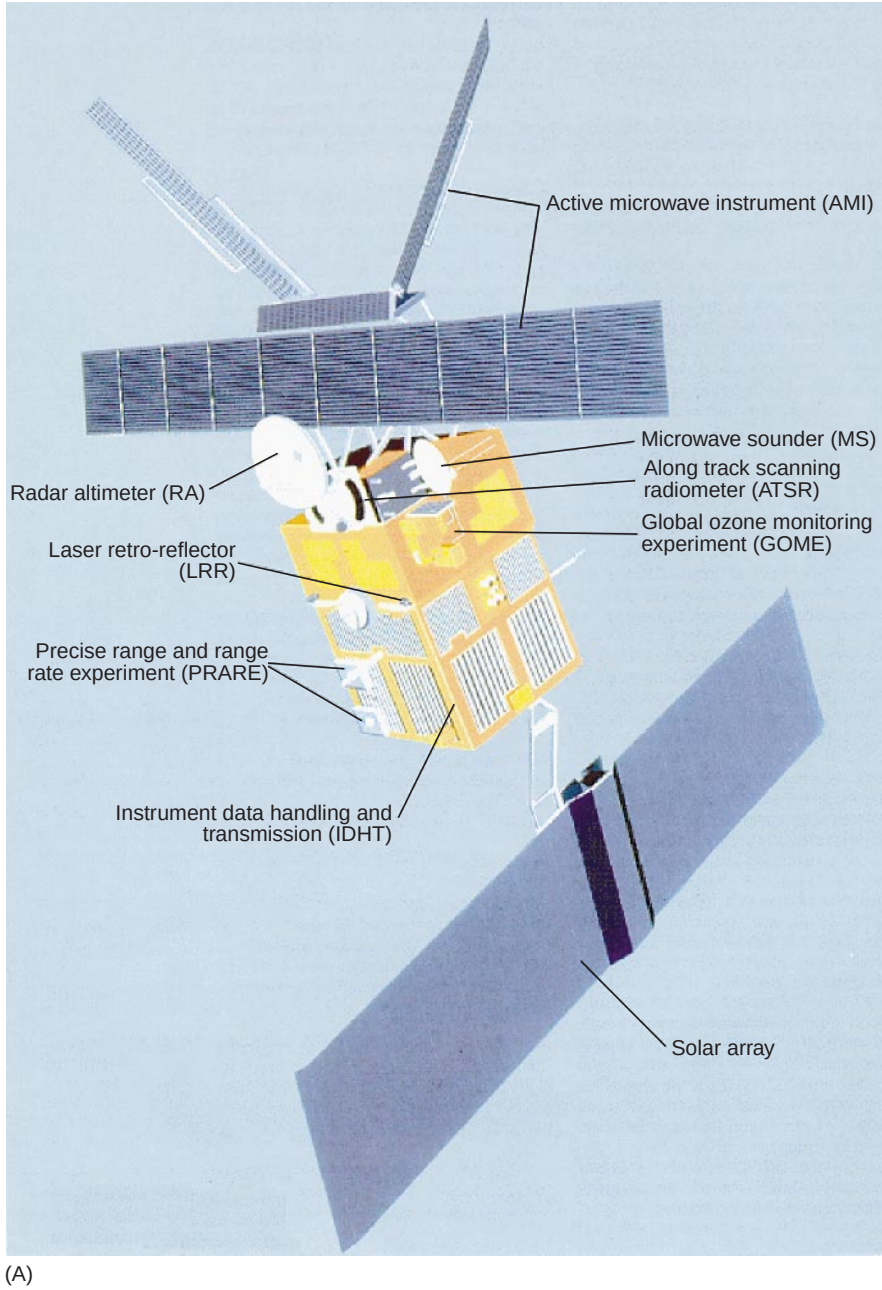

(A)

Figure 1 (A) ERS-1 satellite with two scatterometer waveguide antennas directed upwards. (B) QuikSCAT satellite with parabolic antenna with dual beams pointed downwards.

(B)

Figure 1 *Continued*

The Normalized Radar Cross-section of the Sea

The basis of a scatterometer's ability to measure the near-surface wind vector is the dependence of the normalized radar cross-section of the sea, σ_o, on this vector. This cross-section is defined through the radar equation as follows:

$$P_r = \frac{P_t G^2 \lambda^2 A \sigma_o}{(4\pi)^3 R^4} + P_n \qquad [1]$$

where P_r is the received power, P_t is the transmitted power, G is antenna gain, λ is microwave length, A is the total illuminated area on the sea surface, and R is the range to the surface. P_n is the noise signal due to thermal noise in the components of the system and natural radiation of the earth to the receiving antenna. In a real scatterometer, the received power is reduced below the above level by system losses that must be taken into account. Also, for greater accuracy, the variation of G and R over the scatterometer footprint are taken into account by integration over the footprint. By relating σ_o rather than P_r to the wind vector, the importance of system-specific parameters, P_t, G, R, and λ, are greatly reduced. In fact, σ_o is independent of the first three of these parameters and depends on λ only because the mechanism of backscatter from the sea surface is weakly dependent on λ. Two other system parameters upon which σ_o depends due to the surface scattering mechanism are the incidence angle and the polarization. The strength of backscatter from the ocean surface increases with decreasing incidence angle and depends on the direction of the electric field of the incident radiation, its polarization.

The radar equation must be solved in order to obtain σ_o. This requires a knowledge of P_n, which is usually obtained by sampling only noise signals on a small fraction of the transmitted pulses, typically about 15%. The noise level obtained in this manner is subtracted from P_r and the difference is multiplied or divided by the other quantities which are known. This yields σ_o values that are accurate down to very low signal-to-noise ratios, but that can become negative due to sampling variability. This is an important consideration in the measurement of very low wind speeds.

Figure 2 shows the measured dependance of σ_o on polarization and incidence angle as well as on the wind vector. Two polarizations are indicated in the figure: the electric field vertical on both transmission and reception (VV) and the electric field horizontal on both (HH). These are the two polarizations of importance in scatterometry. The characteristics of σ_o that make it useful for wind vector measurement are obvious from this figure: for any given incidence angle and polarization, it depends on both wind speed and direction. In general the slope of σ_o versus wind speed is smaller at lower incidence angles. The dependence of σ_o on azimuth angle, χ, defined as the angle between the horizontal direction the antenna is pointing and the direction from which the wind comes, has generally been found to fit a three-term Fourier cosine series in χ very well. The relationship between σ_o and incidence angle, θ_i, polarization, p, wind speed, U, and wind direction, χ, is called the geophysical model function. Its general form is taken

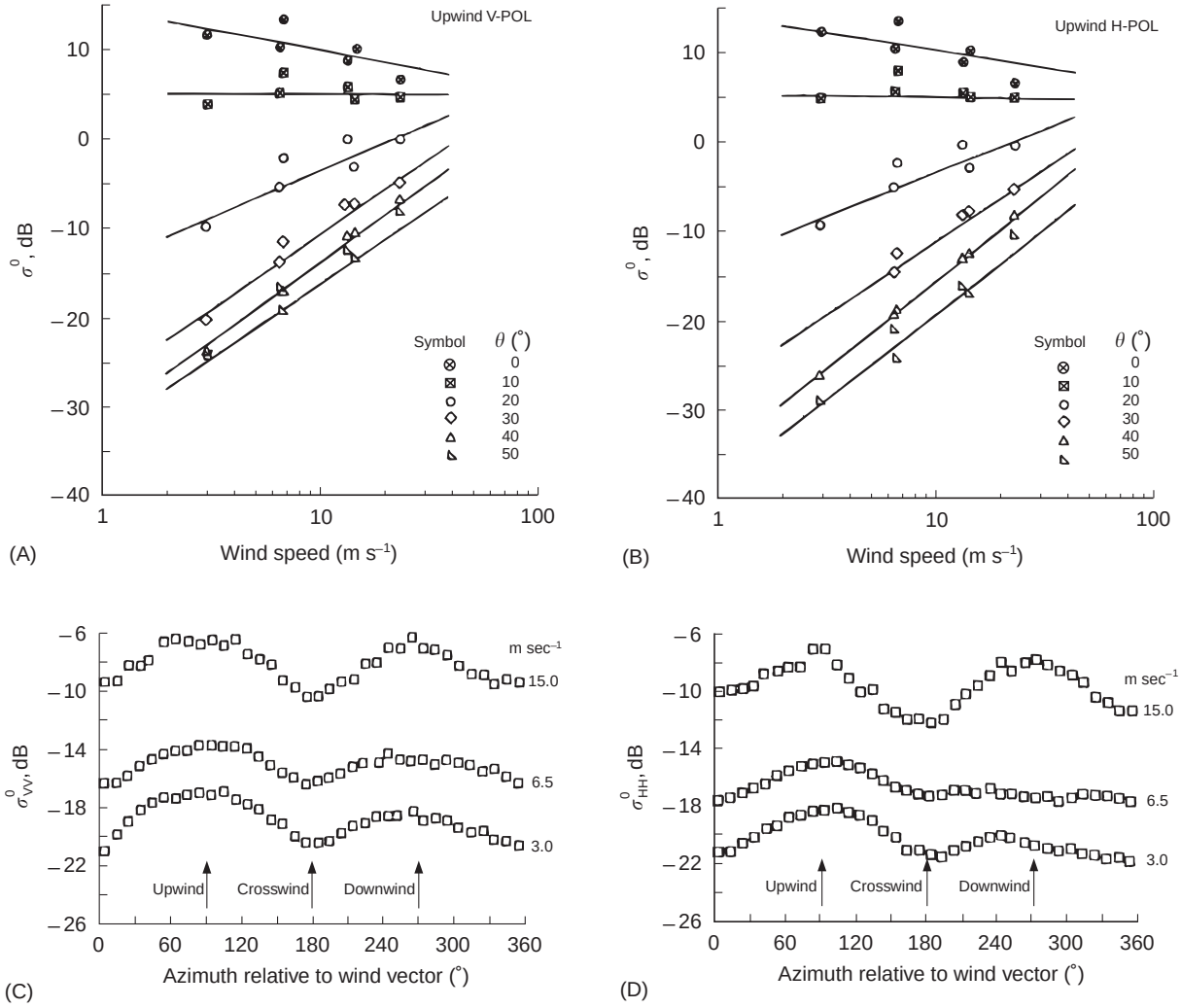

Figure 2 (A) Normalized radar cross section, σ_0 versus wind speed for VV polarization and an upwind look direction (θ is incidence angle); (B) same as (A) for HH polarization; (C) azimuthal dependence of σ_0 for VV polarization and a 30° incidence angle; (D) same as (C) for HH polarization. (Reproduced with permission from Jones WL *et al.* Aircraft measurements of the microwave scattering signature of the ocean. *IEEE Journal of Oceanic Engineering* © 1977 IEEE.)

to be the following:

$$\sigma_o = A_o(U, \theta_i, p) + A_1(U, \theta_i, p)\cos\chi + A_2(U, \theta_i, p)\cos 2\chi \quad [2]$$

Usually the A coefficients are specified in tabular form.

Some characteristics of the dependence of σ_o on χ can be easily discerned in **Figure 2**. Cross-sections measured with the antenna looking nearly perpendicular to the wind direction ($\chi = 90^\circ$ or 270°) are always lower than those measured with the antenna directed upwind ($\chi = 0^\circ$) or downwind ($\chi = 180^\circ$). Furthermore, σ_o is larger when the antenna looks upwind than when it looks downwind, except perhaps for VV polarization at small incidence angles.

Spaceborne Scatterometer Wind Measurements

Given the behavior of σ_o shown in **Figure 2**, a scatterometer fixed on Earth can easily yield the wind vector. If the antenna is rotated and the direction of maximum σ_o is determined, then the level of σ_o in this direction yields the wind speed. In most cases, the direction of maximum σ_o would be the wind direction. The exception to this might be at VV polarization for some incidence angles where the downwind look direction could yield the maximum σ_o. Thus a 180° ambiguity might exist in the wind direction.

Unfortunately this simple technique will not work from satellites because of their high speeds. By the time the antenna rotates one revolution, the satellite has travelled several kilometers, so the footprint on the surface samples many different, widely separated areas. The solution to this problem is to use σ_o values measured in different directions at different times so that nearly the same surface area is illuminated in each direction. **Figure 3** indicates how this might be accomplished in the case of three, fixed stick antennas (**Figure 3A**) and in the case of a rotating antenna with two beams (**Figure 3B**). The first case corresponds to the ERS scatterometers

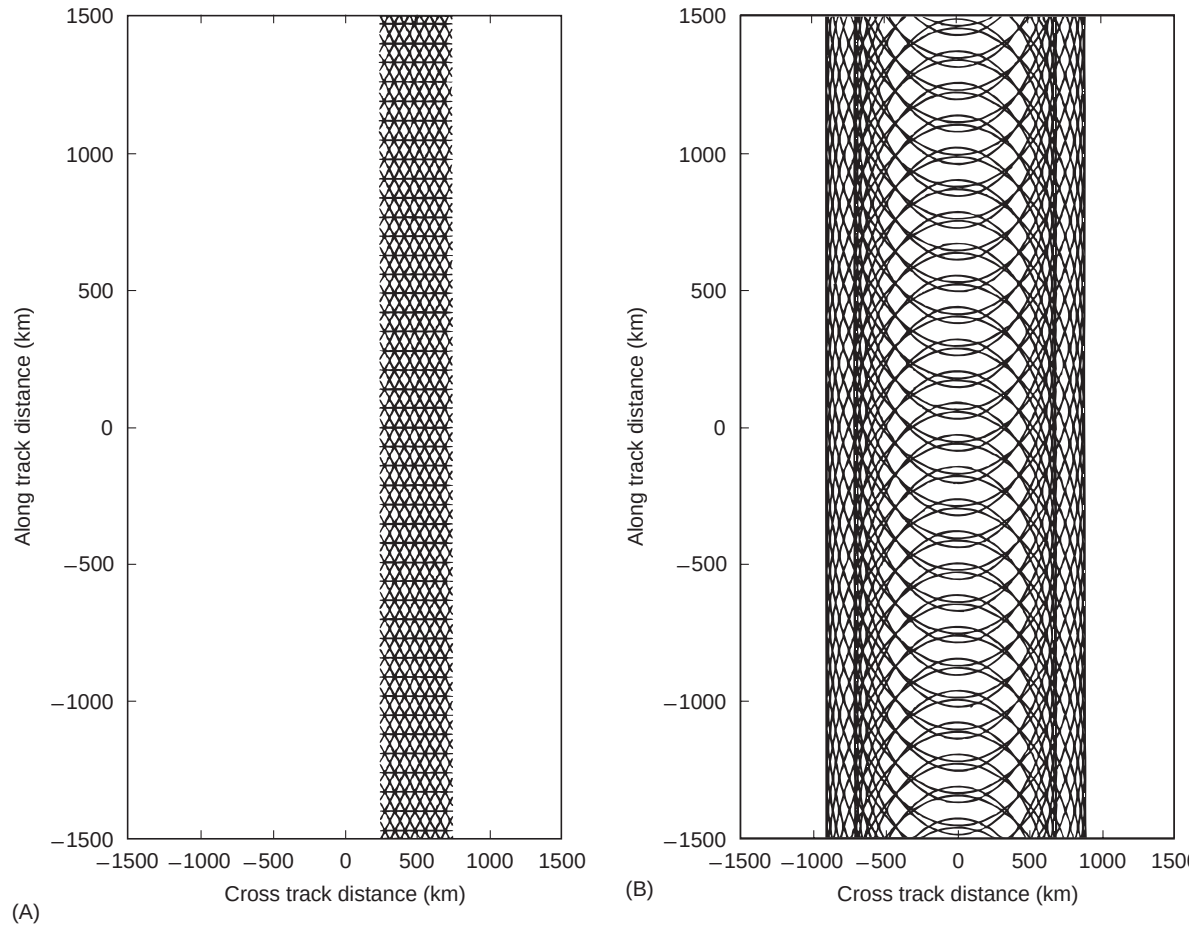

Figure 3 Lines on which scatterometer surface footprints lie showing crossing where multiple look directions occur. Along track distance expanded by a factor of 5. (A) ERS-1/2, (B) SeaWinds.

while the latter corresponds to SeaWinds whose single rotating antenna transmits beams at two different incidence angles. **Figure 3** shows the lines on which the surface resolution cells are located. For clarity, the vertical distance traveled by the satellite has been expanded by a factor of 5 in **Figure 3**. Thus crossings of the lines, where cross-sections can be measured from different directions, are more frequent than indicated in the figure. The two parts of **Figure 3** have the same horizontal scale to emphasize the much wider swath of the SeaWinds scatterometer compared with ERS. For regions of the swath near the center, however, the azimuth angles at which the SeaWinds beam views the surface are nearly opposite or parallel. Furthermore, near the edges, only two nearly parallel looks at a given surface area can be obtained. Estimation of wind speed and direction is consequently more difficult near the center and edge of the swath due to the ambiguous nature of the model function.

The ambiguities inherent in the form of the model function are illustrated in **Figure 4**. The figure shows the angular dependence of σ_o for winds coming from 80°, 180°, 260°, and 345° with respect to north. Each curve maximizes when the antenna is directed into the wind direction. The circles in the figure represent measurements of the cross-section made by an ERS-type scatterometer where the three beams are 45° apart. As the figure shows, winds from 180° and 345° fit the measurements equally well. If the scatterometer had only two beams that were 90° apart, like the Seasat scatterometer, then the other two wind directions, 80° and 260° would also fit the data, provided that the wind speeds were slightly higher for the 260° direction and slightly lower for the 80° direction. Ambiguous wind vectors always exist in the output of scatterometers. Attempts to resolve these ambiguities have ranged from using human analysts to insure consistency of the wind fields to using median filters in which a given wind vector is forced to be in the direction

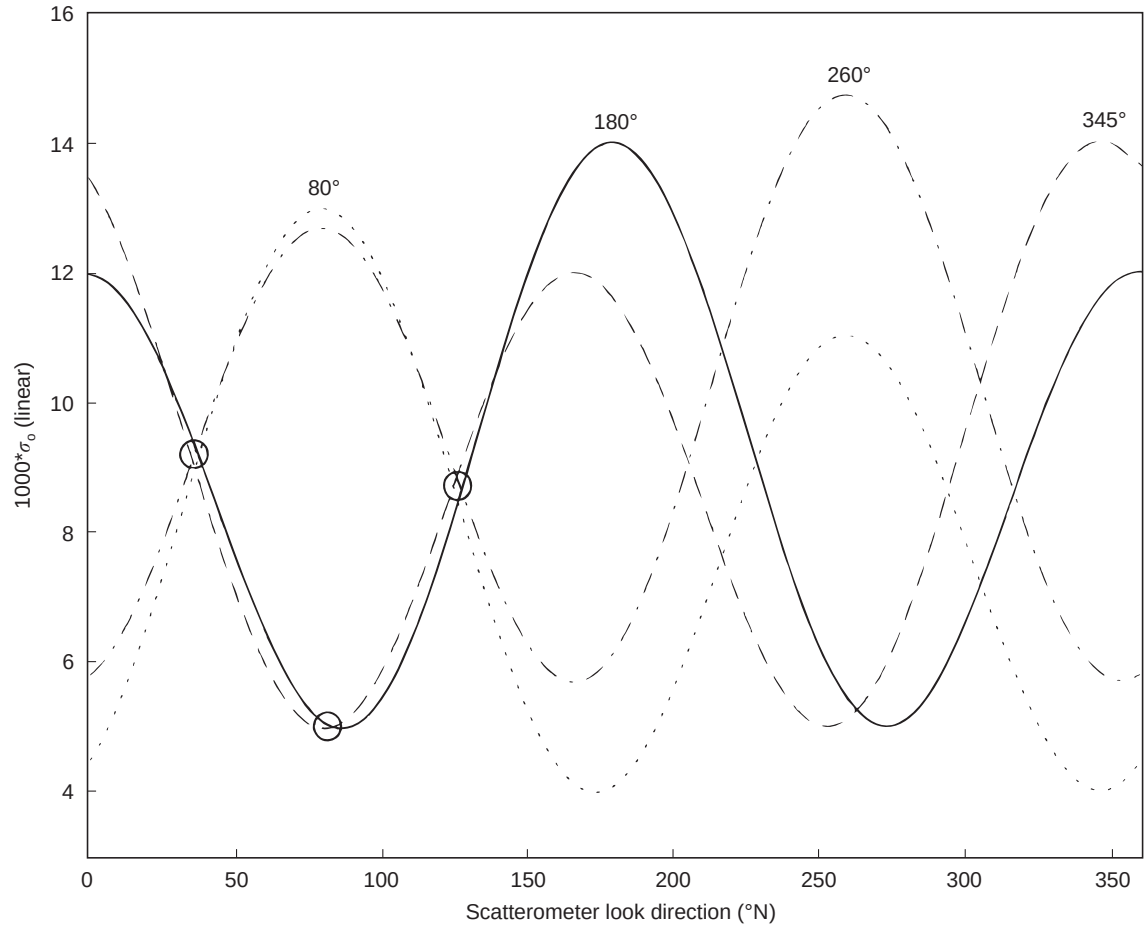

Figure 4 Angular dependence of σ_0 for various wind directions (indicated in the figure). Wind speeds vary little. Circles show possible data points; curves crossing at data points produce ambiguities in wind direction.

of the median of its surrounding vectors. While automatic techniques such as median filtering are now producing skills upwards of 90% in selecting the correct ambiguity, incorrect assignment of vector directions in some locations is still a problem for scatterometry.

Retrieval of the ambiguous wind vectors is accomplished in practice by noting that any single measurement of σ_o is an average of measurements from several scatterometer pulses and therefore has a probability distribution near Gaussian. The variance, δ^2, of this distribution may be determined from the characteristics of the scatterometer, especially its noise level, along with σ_o. Thus the probability of measuring a given σ_o value, call it $\hat{\sigma}_o$, is given by

$$P(\hat{\sigma}_o) = \frac{1}{\sqrt{2\pi\delta^2}} e^{(\hat{\sigma}_o - \sigma_o)^2/2\delta^2} \quad [3]$$

where σ_o is the true normalized cross-section. Since this is unknown in practice, the value of σ_o given by the geophysical model function is used instead.

If all the measured values of $\hat{\sigma}_o$ from every view of the surface that is within the specified resolution of the system (for the NASA scatterometer (NSCAT) with a 50×50 km resolution this could be up to 24) then the joint probability of measuring these values is the product of many Gaussian distributions such as eqn [3]. The wind speed and direction, and therefore σ_o, are then varied to maximize this joint probability. This is the same as minimizing the following objective function:

$$J(U, \chi) = \sum_{i=1}^{N} \left[\ln \delta_i^2 + \left(\frac{\hat{\sigma}_{oi} - \sigma_{oi}(U, \chi)}{\delta_i} \right)^2 \right] \quad [4]$$

Good knowledge of both the geophysical model function and the variances associated with the different looks is essential for a good retrieval.

Calibration

In principle, σ_o values obtained by scatterometers need not be calibrated in an absolute sense; they could simply be related to the surface wind that produced them. In order to cross-check the operation of different scatterometers and to further the development of rough surface scattering theories, however, all scatterometers flown in space have produced normalized radar cross-sections that have been calibrated against a standard target. Usually signals from a geophysical target that has been calibrated by airborne measurements and found to be isotropic are used for calibration of σ_o from spaceborne scatterometers. The Amazon Rain Forest is the most common geophysical target chosen, although areas of Antarctica have also been used.

Calibration and verification of scatterometer winds require an exact definition of the wind that a scatterometer measures. Since a scatterometer really responds to surface roughness, the suggestion has often been made that a scatterometer measures the stress of the wind on the ocean surface rather than the wind vector itself. In fact, a geophysical model function has been developed to relate σ_o directly to the friction velocity, the square root of the stress divided by the density of air. However, to date this procedure has not been adopted by any agency operating a scatterometer. Rather, official winds produced by scatterometers are the winds measured at 10 m above the ocean surface that would yield the same surface stress under neutrally buoyant atmospheric stratification. The only exception was the Seasat scatterometer, whose output winds were specified at a height of 19.5 m above the surface; these are approximately 6% higher than winds at 10 m. Thus wind fields produced by scatterometers are not necessarily the wind fields that a fixed array of *in situ* anemometers would measure, even if they were all at a height of 10 m. Not only are scatterometer wind fields the neutrally buoyant equivalent winds, but evidence is growing that these wind fields are the ones that would be measured under neutral conditions by an anemometer drifting along with the ambient ocean current.

Although physical models of backscatter from the wind-roughened ocean have been developed, they have not proven to be sufficiently accurate to be used as geophysical model functions. Therefore wind retrieval from scatterometers flown to date has been achieved using empirical model functions developed by various means. Experiments have been mounted to relate cross-sections measured by airborne scatterometers to *in situ* measurements of winds converted to neutral conditions. The Europeans noted that if σ_o depends on no other environmental variables than U and χ, then σ_o values measured by three antennas looking in three different directions must fall on a well-defined surface when σ_o values from the three separate antennas are plotted on three orthogonal axes. This observation has allowed them to determine the properties of the geophysical model function to within a constant calibration factor, which was obtained from comparisons with buoy measurements. US geophysical model functions have also been developed by

comparison of cross-sections with buoy measurements and with winds measured by other remote sensing instruments, such as microwave radiometers. Most recently, however, US geophysical model functions have been developed by binning satellite scatterometer σ_o values according to U and χ values produced by numerical weather prediction models. The idea is that errors in the numerical model will cancel out in the mean so that the correct model function can be obtained even in the presence of these errors.

After a model function has been developed by some means, a period of validation of the scatterometer wind fields always follows. Generally scatterometer wind fields are compared with those measured by buoys moored in fixed locations whose anemometer readings have been corrected to 10 m and neutral conditions. As an indication of the accuracy that can be obtained by scatterometers, **Figure 5** shows a comparison of wind speeds and directions produced by NSCAT with winds measured by anemometers on buoys operated by the US National Data Buoy Center (NDBC). To produce the wind speed comparison in **Figure 5A**, buoy wind speeds have been binned into 0.5 m s^{-1} bins and the corresponding NSCAT winds measured near the buoy have been averaged for each bin. The nonzero values of NSCAT wind speed at zero buoy wind speed are known to be a result of comparing magnitudes of vectors whose components are Gaussian distributed so the figure shows good agreement. **Figure 5B** shows the distribution of differences between NSCAT wind directions and buoy wind directions for several different wind speeds and again agreement is good.

Applications of Scatterometry

Further indications of the accuracy and usefulness of data on winds from satellite scatterometers come from studies that compare these winds with, or use them in, atmospheric, oceanic, or climate models to assess the improvements possible through the use of scatterometer winds. Comparisons between wind fields from satellite scatterometers and numerical models have shown that significant differences in these fields often exist. Cyclones predicted by numerical models have been found to disagree in location and intensity with those observed in satellite scatterometry, sometimes by 300 km and 10 mbar or more. The location of the Intertropical Convergence Zone (ITCZ) has been shown to be 1°–2° farther south in NSCAT wind fields than in wind fields predicted by the numerical model of the European Centre for Medium-Range Weather Forecasts (ECMWF). Furthermore, the ITCZ observed by NSCAT was stronger and narrower than that predicted by ECMWF. An example of the differences that can occur between scatterometer wind vectors and those of numerical models is given in **Figure 6A**. Here NSCAT measurements in the South China Sea are compared with predictions of the numerical model of the National Centers for Environmental Prediction (NCEP). Obviously the fields can be quite different.

In the South China Sea, the Princeton Ocean Model (POM) was run using wind fields from NSCAT and from NCEP, some of which are shown in **Figure 6A**. The results indicate significant differences in the output of the POM depending on the wind field used, although these differences were generally smaller than those of the wind fields themselves. This is illustrated in **Figure 6B**, which shows surface currents predicted by POM for the two different wind fields and their differences. While this study did not assess which POM prediction was the most accurate, other studies have indicated that the predictions of ocean models and coupled atmosphere–ocean models using scatterometer wind fields agreed with observations better than those using other wind fields. Comparisons of sea levels predicted by the modular ocean model (MOM) with those of the TOPEX/Poseidon radar altimeter have indicated that more accurate predictions are achieved using ERS-1 wind fields than using NCEP fields. Similarly, prediction of the 1997–98 El Niño by the Lamont-Doherty Earth Observatory model has been shown to be improved by using NSCAT wind fields rather than the surface observations collected by Florida State University (FSU). This is illustrated in **Figure 7**. Here sea surface temperature anomolies (with respect to FSU climatology) in the eastern tropical Pacific predicted by the model with FSU and NSCAT wind fields are compared with those actually observed in 1997 and 1998. NSCAT wind fields have improved the prediction.

Limitations and Improvements

The examples above indicate the usefulness of satellite scatterometry in oceanic and atmospheric modeling. However, limitations still exist in the satellite wind fields which make them less useful than they could be. Ambiguities have been mentioned earlier. The temporal and spatial sampling patterns inherent in the data collection of individual satellites can obscure geophysical effects that occur on spatial scales less than about 200 km and temporal scales less than a day or two. This effectively limits the

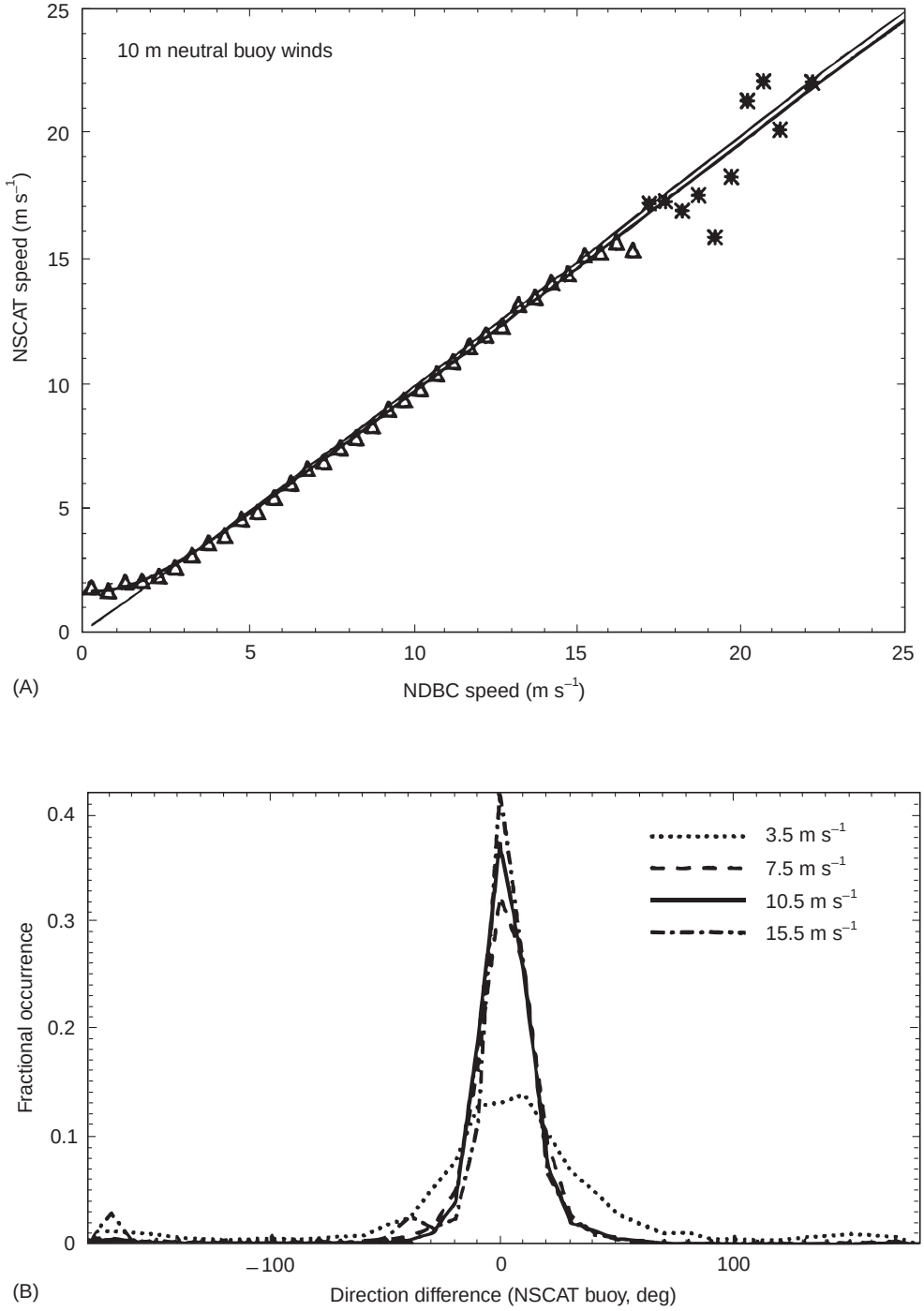

Figure 5 (A) Sample mean NSCAT wind speeds in 0.5 m s^{-1} buoy wind speed bins. All NSCAT measurements were located within 50 km and 30 min of buoy measurements. Triangles denote >100 NSCAT measurements in the mean; asterisks denote 5–99 samples. (B) Distributions of directional differences (NSCAT buoy) for 1 m s^{-1} buoy wind speed bins centered on the indicated wind speeds. (Reproduced with permission from Freilich and Dunbar, 1999.)

application of satellite scatterometry to low-frequency, large-scale events. Interpolation of the raw data can reduce this problem somewhat but may introduce false signals. The obvious way to alleviate the problem is to put fleets of satellite scatterometers into orbit, an idea that may not be completely impossible in this day of smaller, cheaper satellites.

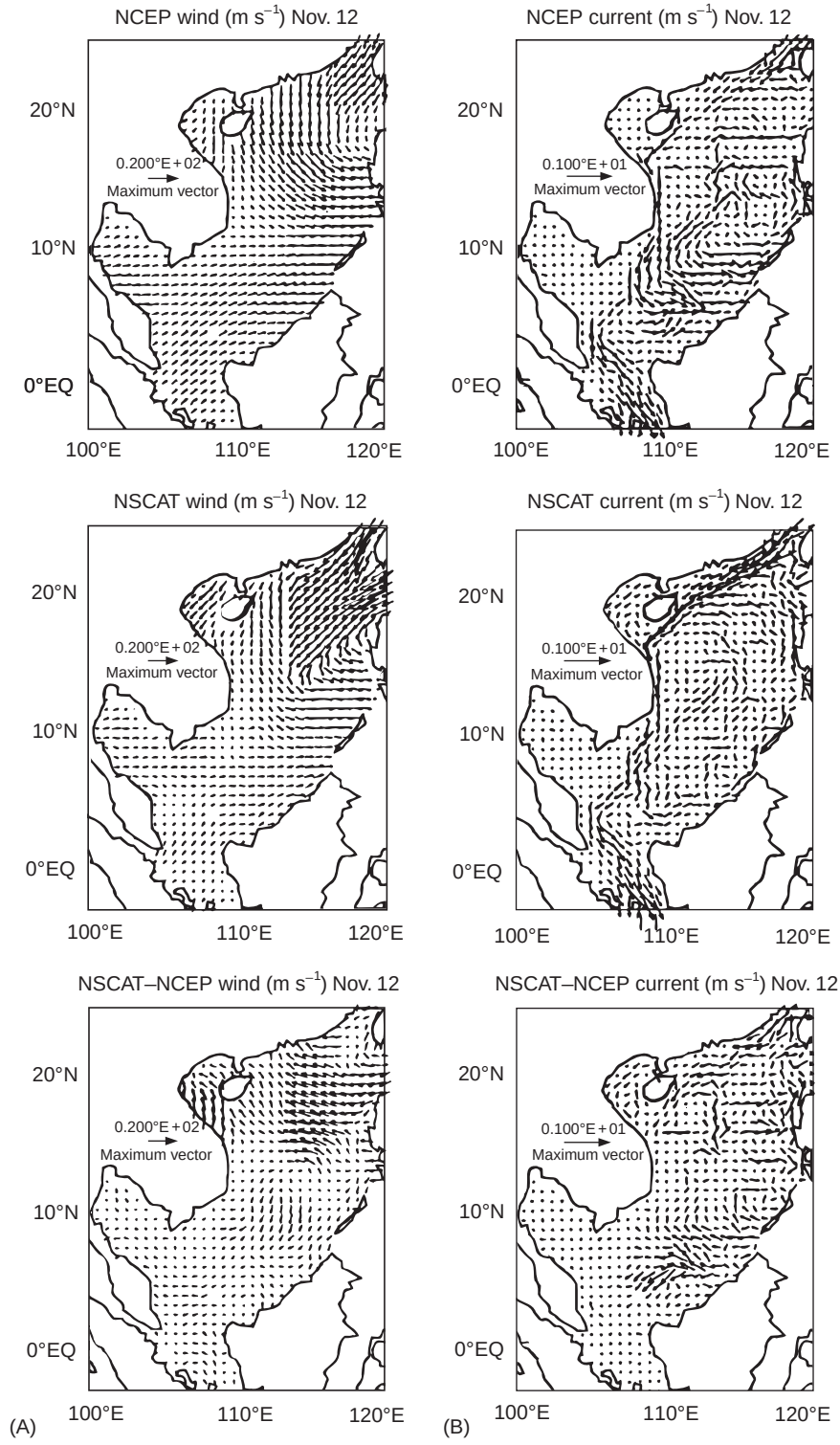

Figure 6 (A) NCEP and NSCAT wind vectors in the South China Sea and their differences. (B) Surface currents in the South China Sea from NCEP model under NCEP and NSCAT wind forcing. (Reproduced with permission from Chu *et al.*, 1999.)

Another limitation on satellite scatterometry that has been observed many times is the mismeasurement of surface wind fields in the presence of rain. Without an accompanying microwave radiometer, it is difficult to ascertain from scatterometer measurements alone when rain is occurring on the surface.

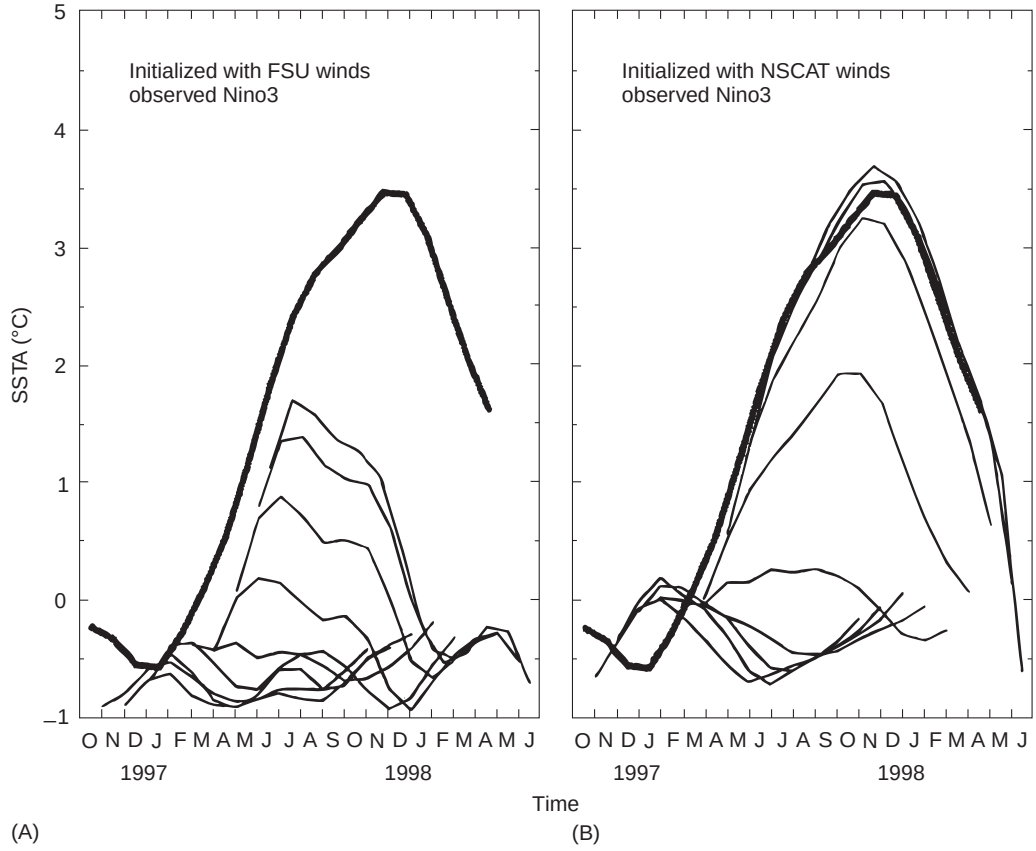

Figure 7 Forecasts of sea surface temperature anomalies in the eastern tropical Pacific for the 1997–98 El Niño by the Lamont-Doherty Earth Observatory model using (A) Florida State University winds and (B) NSCAT winds. Heavy curves are observations; other lines are predictions made at various times (Reproduced with permission from Chen *et al.*, 1999.)

Since heavy rainfall can attenuate a Ku-band scatterometer signal by more than a factor of 10 every kilometer, serious mismeasurement of surface wind fields can occur when rain is present. Furthermore, microwave return from the sea surface is also changed by rainfall, and this change is not well understood. Measurements indicate that σ_o becomes more isotropic in the presence of rain, and this effect is being utilized in an attempt to develop a rain flag from scatterometer data alone. Such a flag would allow users to determine when rain effects might be present in scatterometer data, but not what the proper wind vectors are.

Winds below $3\,\mathrm{m\,s^{-1}}$ are difficult to measure accurately using satellite scatterometry. Present geophysical model functions are smoothly decreasing functions of wind speed that are nonzero even at zero wind speeds. The Europeans have chosen not to provide wind speed estimates below $3\,\mathrm{m\,s^{-1}}$ using their ERS scatterometers. Recent studies have shown that, in addition to the directional variability inherent in low winds, microwave backscatter is virtually zero below some threshold wind speed in the neighborhood of $2\,\mathrm{m\,s^{-1}}$ to $4.5\,\mathrm{m\,s^{-1}}$, depending on incidence angle and water temperature. Variability of the wind over the surface footprint of the scatterometer, however, obscures this threshold in most satellite scatterometry measurements. The geophysical model function at these low wind speeds therefore appears to depend on both the mean wind vector over the footprint and its variability. Suggestions for improving low wind speed measurements have included specifying a variability-dependent model function that depends on geographic region and season, as well as using details of the probability distribution on σ_o. Implementation of such suggestions in future retrieval schemes offers hope of improving low wind speed measurements.

Finally, high wind speeds have also proven to be a problem for scatterometry. Recent studies indicate that σ_o increases less rapidly with wind speed above about $25\,\mathrm{m\,s^{-1}}$ than current model functions predict. The result is that wind speeds above this value tend to be underestimated in scatterometry wind retrievals. Proposals have been offered for improved

high wind speed model functions based on simultaneous scatterometry/radiometry measurements from aircraft flying through hurricanes. Implementation of such model functions promises to yield better wind retrievals at high wind speeds.

Conclusion

Satellite-based microwave scatterometry is a mature technology that has proven itself capable of yielding global oceanic wind speeds of unprecedented accuracy and spatial coverage. Satellites currently in orbit and planned for future missions promise a continuous long-term series of global wind measurements that can aid in climate studies. Based on the time-series presently available, satellite scatterometer measurements have proven themself capable of improving present oceanographic and atmospheric models. Future improvements in scatterometry promise to make this technology even more valuable in studying the dynamics of the atmosphere and oceans.

See also

Aircraft Remote Sensing. Air–Sea Gas Exchange. Heat and Momentum Fluxes at the Sea Surface. History of Satellite Oceanography and Introductory Concepts. Satellite Altimetry. Satellite Measurements of Salinity. Satellite Passive Microwave Measurements of Sea Ice. Satellite Remote Sensing SAR. Satellite Remote Sensing of Sea Surface Temperatures. Sensors for Mean Meteorology. Sensors for Micrometeorological Flux Measurements. Surface, Gravity and Capillary Waves. Wave Generation by Wind. Wind and Buoyancy-forced Upper Ocean. Wind Driven Circulation.

Further Reading

Brown RA and Zeng L (1994) Estimating central pressures of oceanic midlatitude cyclones. *Journal of Applied Meteorology* 33: 1088–1095.

Chen D, Cane MA and Zebiak SE (1999) The impact of NSCAT winds on predicting the 1997/1998 El Niño: A case study with the Lamont-Doherty Earth Observatory model. *Journal of Geophysical Research* 104: 11322–11327.

Chu PC, Lu S and Liu WT (1999) Uncertainty of South China Sea prediction using NSCAT and National Centers for Environmental Prediction winds during tropical storm Ernie, 1996. *Journal of Geophysical Research* 104: 11273–11289.

Donelan MA and Pierson WJ (1987) Radar scattering and equilibrium ranges in wind-generated waves with application to scatterometry. *Journal of Geophysical Research* **92**: 4971–5029.

Fisher RE (1972) Standard deviation of scatterometer measurements from space. *IEEE Transactions Geoscience Electronics* GE-10: 106–113.

Freilich MH (1997) Validation of vector magnitude datasets: effects of random component errors. *Journal of Atmospheric and Oceanic Technology* 14: 695–703.

Freilich MH and Dunbar RS (1999) The accuracy of the NSCAT 1 vector winds: Comparisons with National Data Buoy Center buoys. *Journal of Geophysical Research* 104: 11231–11246.

Fu Lee-Lueng and Yi Chao (1997) The sensitivity of a global ocean model to wind forcing. A test using sea level and wind observations from satellites and operational wind analysis. *Geophysical Research Letters* 24: 1783–1786.

Graf J, Sasaki C, Winn C *et al.* (1998) NASA scatterometer experiment. *Acta Astronautica* 43: 397–407.

Jones WL, Schroeder LC and Mitchell JL (1977) Aircraft measurements of the microwave scattering signature of the ocean. *IEEE Journal of Oceanic Engineering* OE-2: 52–61.

Kelly KA, Dickinson S and Yu Z (1999) NSCAT tropical wind stress maps: implications for improving ocean modeling. *Journal of Geophysical Research* 104: 11291–11310.

Moore RK and Pierson WJ (1996) *Measuring Sea State and Estimating Surface Winds from a Polar Orbiting Satellite*. In: Proceedings of the International Symposium on Electromagnetic Sensing of Earth from Satellites, Miami Beach, FL, 1966.

Moore RK and Fung AK (1979) Radar determination of winds at sea. *Proceedings of the IEEE* 67: 1504–1521.

Naderi FM, Freilich MH and Long DG (1991) Spaceborne radar measurement of wind velocity over the ocean – An overview of the NSCAT Scatterometer system. *Proceedings of the IEEE* 79: 850–866.

Pierson WJ Jr (1983) The measurement of the synoptic scale wind over the ocean. *Journal of Geophysical Research* 88: 1682–1780.